-RESEARCH PAPER-

International Journal of Mining and Geo-Engineering

IJMGE

IJMGE 55-2 (2021) 145-150 DOI: 10.22059/IJMGE.2020.288862.594825

Effect of Rock Joint on Boreability of TBM at Northern Section of Kerman Water Conveyance Tunnel

Morteza Khosravi [a, *], Ahmad Ramezanzadeh [a], Shokrollah Zare [a]

[a] *Faculty of Mining, Petroleum & Geophysics Engineering, Shahrood University of Technology, Shahrood, Iran*

Article History:

Received: 13 September 2019,
Revised: 28 April 2020,
Accepted: 06 May 2020.

ABSTRACT

Nowadays, Tunnel Boring Machines (TBM) are widely used around the world on account of their high rate of excavation, little impact on the surrounding rock, and their high safety standards. The rock mass boreability is considered as one of the main parameters in evaluating the TBMs' performance in jointed rock masses. Boreability is a parameter reflecting the interaction between the rock mass and cutting tools. This paper aims to render an account of the effect of Joints Geometrical Parameters on the boreability by use of a database prepared to utilize the data (TBM operation and geological parameters) collected from Kerman Water Conveyance Tunnel projects in Iran. For this purpose, the joint parameters (orientation, spacing, persistence) affecting the boreability have initially been investigated. Then, the total fracturing factors (Bruland) and Persistence classification were used to investigate the effects of all three parameters on the boreability. The results showed that the boreability is also increased by increasing the joint persistency. Besides, the effect of fracturing factor ($K_{s\text{-}total}$) on boreability increases by increasing the joint persistency. In this paper, a new parameter called "Rock Joint Index"(RJI) is also presented according to the analysis performed on the database. The boreability value estimated based on the RJI shows a good agreement with the actual penetration rates.

Keywords: *Joint Geometrical Parameters, Jointed Rock Mass, Penetration Rate, Rock Mass Boreability, Tunnel Boring Machines (TBM)*

1. Introduction

Prediction of the penetration rate of a TBM is an important issue in the planning and cost estimates of such tunneling projects. In a tunneling project, many parameters and factors influence the penetration rate of the tunnel boring machine and the rock boreability. In this regard, the most important parameters are divided into three main groups including the parameters of the rock mass, parameters of the intact rock, and operating parameters of the TBM [1]. Jointed parameters are considered as the most important parameters of the rock mass that play an important role in the boreability of the rock mass. The investigation results show that spacing and orientation have the greatest impact on boreability amongst the joint parameters. When a jointed rock mass is excavated using TBM, the effect of the joint orientation on the penetration of the disc cutter is influenced by the angle between the tunnel axis and the dip of the joint (α). Also, it is affected by the angle between the orientation of the disc cutter rotation and the trace of joint placed on the face (β) [2] (Figure 1).

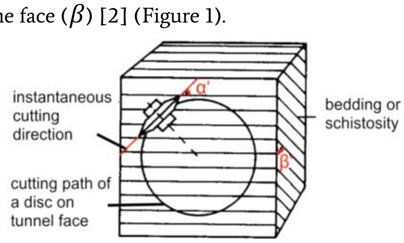

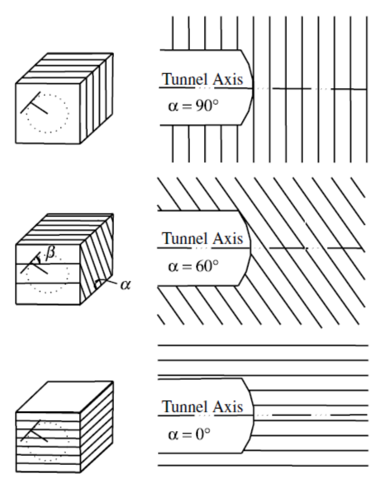

Fig. 1. Effect of joint orientation on TBM penetration [2]

The effect of the joint orientation as an important factor affecting the penetration rate has been studied by many researchers using numerical modeling methods. Gong and Zhao (2005) investigated the orientation effect of a single joint set on the penetration rate. According to the modeling results, the increase in the angle between the joints and tunnel axis up to 60 degrees gives rise to the increase and subsequent decrease of the penetration rate [3]. Therefore, the maximum penetration rate occurs at 60° angle. According to Paltrinieri (2015), the joints parallel to the tunnel axis have the minimum effect on the TBM performance, and a 60-degree orientation along the tunnel axis will effectively increase the

* Corresponding author. Tel: +98-9126455221, *E-mail address:* mortezakhosravi80@gmail.com (M. Khosravi).

penetration rate [4]. Spacing is another joint parameter that affects the penetration rate. Investigations indicate that the effect of discontinuity depends highly on the rock type. According to the results, the slate has had the highest increase in the penetration rate. So, it can be said that this type of rock has the highest effect on the penetration rate. However, the orientation of discontinuities for all rock types affects grinding even more than the discontinuity spacing [5]. Gong and Zhao (2006) studied the effect of joint spacing ranging between 10 and 500 mm on the penetration rate. Besides, the penetration rate decreases by increasing the joints spacing according to the modeling results [6]. Sharifzadeh and Iranzadeh studied the effects of joint set spacing and orientation on TBM performance. According to this study, the critical angle of the joint set with the potential of the maximum intrusion is between 45 to 60 degrees. Furthermore, they concluded that the joint set angle has more effect on the process of rock chip production than the spacing [7]. Bejari et.al studied the simultaneous effect of the joint orientation and spacing on the single disc cutter using the Discrete Element Method (DEM). The results showed that the TBM penetration rate decreased by increasing the joints spacing in a joint orientation [8]. Bejari and Khademi studied the effect of joints spacing and orientation on the efficiency of TBM cutting in the jointed rock mass using the DEM simulation. The analysis results showed that the efficiency of TBM decreases by the increase of the joints spacing with a specific orientation [9]. The geotechnical parameters of the joint including the surface quality, filling, fraction, spacing, and orientation affect the penetration rate, but their influence is less than that of the spacing and orientation [6]. In this study, we have investigated the effect of the joint orientation, spacing, and persistence on boreability using field data obtained from the Kerman Water Conveyance Tunnel Project in Iran. Then, based on the results, a new parameter called "Rock Joint Index"(RJI) is introduced.

2. Kerman Water Conveyance Tunnel

Kerman Water Conveyance Tunnel was designed in the north-south direction. The tunnel is 38 km long with a diameter of 3.90 m. The main objective of this project is to transfer water from Safa Dam to Kerman province.

This tunnel was divided into two sections: the northern section (Golzar part) and the southern section (Ganjan part) each of which has a length of 19 km. The northern portal of the tunnel is located at 2370 meters above sea level, and 50 km south-east of Kerman. The southern portal of tunnels is located at el. 2404 meters above sea level and about 15 km from the Raber area [10]. This tunnel is currently under construction using two double shields (DS) TBMs. The specification of TBM in the northern section is presented in Table 1.

Table 1. Specification of TBM in the northern section [10]

Parameters	Value
Machine type	Hard rock double shield
Bore diameter	4.7 mm
Number of disc cutters	27 items
Disc cutters diameter	19 inch
Stroke length	1.3m
Max Thrust force	16913 KN
Max torque	1725 KNm

The rock mass of the northern section of the tunnel belongs to Precambrian Era. This section is constituted by different sedimentary and volcanic rock sets. The northern section includes the Cenozoic magmatic arc. The oldest sediments of this area belong to the Upper Cretaceous flysches, and its youngest deposits are the recent sediments. The blocks of this area are have been classified based on faults that their activities have continued until now. The engineering geological units in this study have been defined as per BGD (Basic Geotechnical Description) classification. The physical and mechanical characteristics of different units have been investigated using field sampling and laboratory studies. The results have been used for separating the engineering geological units and preparing the engineering geologic cross-section. The study area has been divided into five geologic units as presented in Table 2.

The geological profile of the tunnel direction (study area) is shown in Figure 2.

Table 2. Geological units of the study area [10]

N	Geological units	Dominant lithology	Structure
1	RT1	Andesite	Blocky to mass
2	RT2	Basalt	
3	RT3	Andesite-Basalt	
4	RT4	Diabase	Blocky
5	RT5	Dacite	

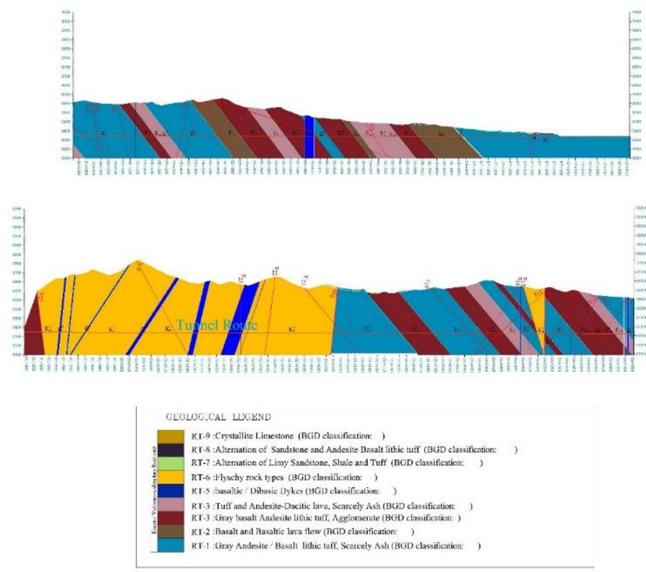

Fig. 2. Geological profile of the tunnel direction (study area) [10]

3. Tunneling data acquisition

A database comprised of the rock geomechanical parameters and TBM operation parameters for 7 kilometers of Kerman Water Conveyance Tunnel was prepared to investigate the joint effect on the boreability within the jointed rock mass. To have more accuracy in this investigation, sections of the tunnel have been selected with the same geological unit, overburden differences of less than 25 meters with the same TBM operator, and disc cutters. In these sections, only the dip and dip direction of the joints have been changed. In addition, the two operating parameters of TBM (thrust and torque) are almost equal. The number of boring strokes under the analyses and geomechanical parameters are shown in Table 3.

Table 3. Number of boring strokes and geomechanical parameters

Meters of tunnel	Number of boring strokes	Geological Type	UCS (Mpa)	BTS
36634	640	RT3 (andesite- basal)	180	20
36321	881		110	17
35240	1753		160	17
34760	1979		120	19
35364	1617	RT1 (Andesite)	160	15
35550	1474		100	11

The TBM operation parameters including the penetration rate, thrust, and torque of every stroke have been recorded in the data recording system. This system could record parameters every 5 seconds. The maximum, minimum, and average values of the TBM operation parameters in the excavation of each boring stroke have been presented in Table 4.

Table 4. TBM operation parameters

Number of boring strokes	penetration rate (mm/rev)			Thrust (KN)			Torque (KN.M)		
	Max	Min	Ave	Max	Min	Ave	Max	Min	Ave
640	9.5	3.6	7.1	4461	3217	3975.7	1076.2	362.2	750.8
881	12.4	7	9	4297	3438	3901.3	1069.3	469.1	753
1474	9.1	5.1	6.5	5225	4198	4760	724	369	536
1617	7.5	4.5	5.8	5277	4178	4800	731	258	488
1753	9.9	5.6	7.78	5572	4493	5070	941	331	623
1979	13.8	7.7	9.5	5409	4179	4769	1003	465	658

4. Effect of Geometric Parameters of Joint on boreability

The behavior of jointed rock mass is influenced by the system discontinuity characteristics. The discontinuity characteristics of the rock mass system include dip, dip direction, spacing, persistence, aperture, filling, and discontinuity surfaces. To collect the joints information for Kerman Water Conveyance Tunnel, surface surveying has also been performed apart from the exploratory excavation at the tunnel axis. During the exploratory excavation, accurate characteristics of the joints including the shape of the joint surface, the angle of joint to the excavation axis, aperture, type of filling, persistence, and weathering of the joint surface have been collected during the core drilling. At first, the data related to the bore joint studies were estimated for each formation separately. Then, it was observed that some characteristics of the surface of rock mass discontinuities at surface traces were somehow different from those corresponding to the depth of the rock mass. In particular, two factors including weathering degree and discontinuity fraction at the depth of the rock mass would have different conditions compared to the surface. These data would be corrected and updated using the cores extracted during the excavation. The characteristics of the joint sets have been shown in Table 5.

Table 5. Characteristics of joint sets in strokes

Number of boring strokes	Joint sets	Dip	Dip Direction	Aperture (mm)	Spacing (m)	Persistence (m)
640	1	61	214	2.1	1.48	3.5
	2	77	135	2.6	1.27	3.5
	3	55	40	0.5	0.4	2
881	1	46	232	2.5	0.67	8
	2	67	58	2.7	1.5	4.4
	3	58	158	1.8	1.26	2.9
1474	1	48	218	2.3	0.58	5
	2	82	95	1.3	0.83	3.6
	3	70	175	1.34	1.06	3.3
1617	1	76	117	3.5	0.65	3.7
	2	60	12	1.3	1	2.6
	3	67	203	1.1	1.08	3.07
1753	1	13	192	3	3	2
	2	82	312	2	0.55	3
	3	72	218	3	3	4
1979	1	85	163	1.7	1.35	4.7
	2	73	359	2.93	1.3	4.6
	3	67	268	2.64	1.2	3.8

Changes in the joint plane angle, aperture, spacing, and persistence at both strokes, have been investigated with variable penetration rates in order to study the effects of each joint parameter on the boreability. The angle of the joint plane with tunnel axis has been used to investigate the effect of joint plane angle, which is computed based on the relationship proposed by Bruland (1999) and Macias (2016) [11].

$$\alpha = \left|\mathrm{Arcsin}(\sin\alpha_f \times \sin(\alpha_t - \alpha_s))\right| \quad (1)$$

where:

α is the angle between the tunnel axis and the joint plane, α_f is the dip angle of the joint plane, α_s is the joint angle, and α_t is the axis azimuth of the tunnel. The computed angles for each joint have been presented in Table 6.

Table 6. The angle between the tunnel axis and the plane of joint

Alpha (α)	Number of boring strokes					
	881	640	1474	1617	1753	1979
1	18	28.7	4.6	10.4	2.6	1
2	34	31.3	26.7	20.4	35.9	17
3	51	42.9	78.5	59.3	47.4	66.8

In continuation, the variation of joint parameters with the penetration rate for both strokes has been drawn with similar conditions (Fig 3, 4, 5).

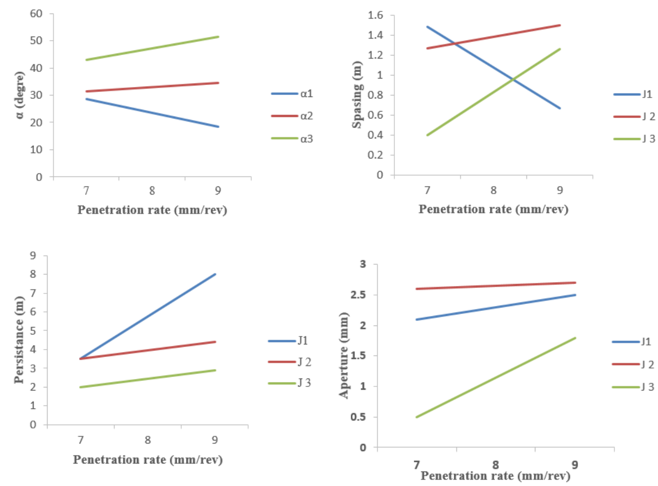

Fig. 3. Variation of geometric Parameters of Joint with penetration rate for strokes 640 & 881

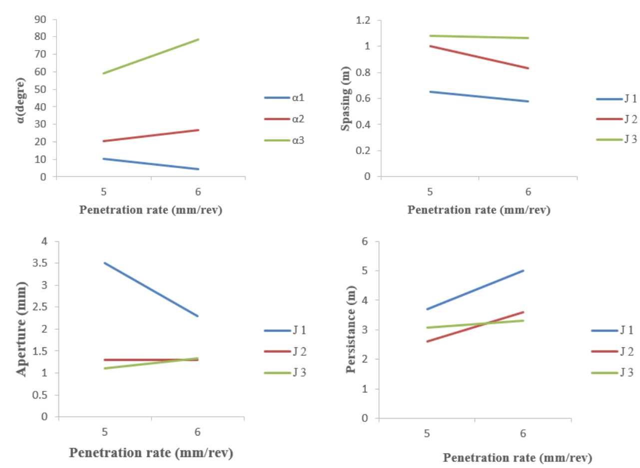

Fig. 4. Variation of Geometric Parameters of Joint with penetration rate for strokes 1474 & 1617.

In order to investigate the effect of joint parameters on the penetration rate, first, the effects of two parameters of joint plane angle and spacing have been studied using the Norwegian classification system. It is required to have two important parameters of discontinuity class (NTH class) and total fracturing factor ($K_{s\text{-}total}$) to classify the rock mass in the Norwegian classification system in estimating the rock mass boreability characteristics. This classification was presented initially by Blindham (1979) at NTNU University and then was updated and completed by Bruland (1998) and Macias (2016) [11, 12]. The classification according to the degree of fracturing and jointed rock mass is based on the joint spacing (Table 7).

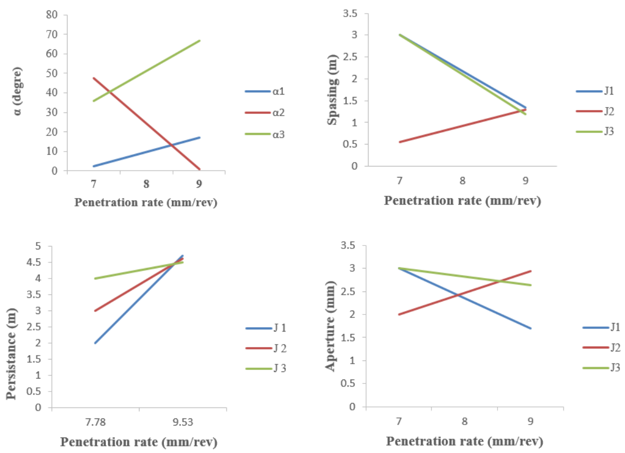

Fig. 5. Variation of Geometric Parameters of Joint with penetration rate for strokes 1753 & 1979

Table 7. Classification of degree of fracturing and jointed rock mass [11]

Fracture Class(Sf)	The average spacing between fractures (cm)	Range class (cm)	Degree of fracturing
0	∞	480-∞	Non-fractured
1	320	240-480	Extremely low
2	160	120-240	Very low
3	80	60-120	Low
4	40	30-60	Medium
5	20	15-30	High
6	10	7.5-15	Very high
7	5	4-7.5	Extremely high

The fracturing factor (Ks) for each joint has been obtained after assigning the class of fraction, using the angle of the joint plane and class of joint that is in accordance with Figure 6.

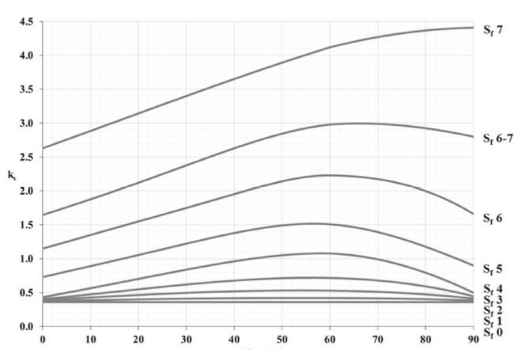

Fig. 6. Rock mass fracturing factor (ks) as a function of the angle between the tunnel axis and the fractures [10]

Finally, the total fracturing factor ($K_{s\text{-total}}$) was obtained using the following equation.

$$K_{s-total} = \sum_{i=1}^{n} K_{si} - (n-1)0.36 \quad (2)$$

In continuation, variations of Ks and $K_{s\text{-total}}$ with the penetration rate have been drawn to investigate this issue (Fig 7, 8).

At the next step, the joint plane angle and spacing as well as the presented classification using rock mechanics principles have been used in order to account for the effect of joint persistence (Table 8).

Table 8. Persistence classification [13]

Class	Persistence (m)
1	Less than 1 m
2	Between 1 and 3 m
3	More than 3 m

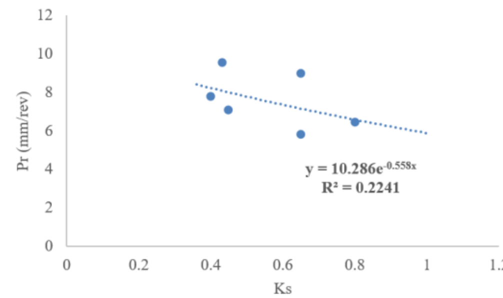

Fig. 7. The variance of Ks with the penetration rate

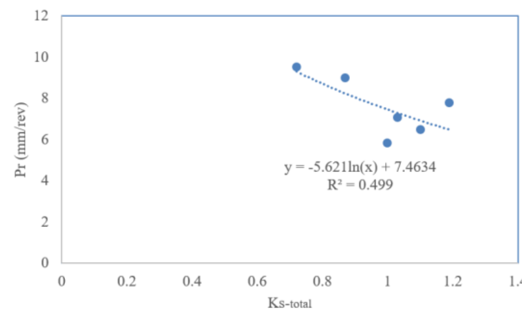

Fig. 8. The variance of $K_{s\text{-total}}$ with the penetration rate

The variations of penetration rate and the total fracturing factor have been drawn according to the above table (Fig 9).

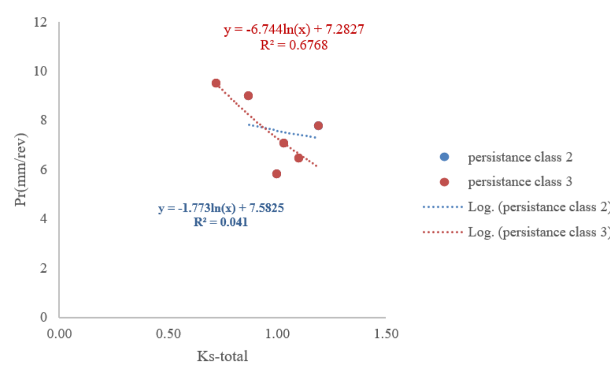

Fig. 9. The variance of $K_{s\text{-total}}$ with the penetration rate

5. Discussion

Having compared the variations charts of each parameter with the penetration rate, it can be observed that:

1. In some cases, the penetration rate increases following the increase of the joint plane angle with the tunnel angle, and in some cases, the penetration rate increases by the decrease in this angle. Therefore, we cannot determine a specific relationship between the joint plane angle and the penetration rate. in addition, with regard to the existing difference in the range of variation of angles, we cannot determine a specific range for the angle to define a relationship between angle variation and the penetration rate.
2. As for the joint spacing, it can be observed that with an increase in the joint spacing per strokes 640 and 881, there would be an increase in the penetration rate. But for the strokes 1753 and 1989, we observe that the penetration rate increases following a decrease in spacing. Therefore, we cannot determine a specific relationship between the joint spacing and the penetration rate.
3. By comparing the changes in the joint persistence parameters with the penetration rate, it is observed that the penetration rate

increases following an increase in the persistence. This shows that with an increase in the joint persistence, a wider contact is formed between the boring head disc cutters and the joint, which will increase the penetration rate of the machine. The study carried out on the relationship between volumetric joint count and the penetration rate reveals that the penetration rate increases when increasing the volumetric joint count. This issue also proves that the penetration rate increases by the increase in the number of joints surfaces.

4. The fracturing factor which is a combination of two parameters, i.e. the joint plane angle and spacing, has an adverse relationship with the penetration rate. As seen in Figure 8, the fracturing factor increases by the increase in the fracturing class (decrease in the joint spacing) and joint plane angle. By adding the joint persistence parameter in Figure 10, it is observed that by an increase in the joint persistence, the convergence factor of the relationship between penetration rate changes by total fracturing factor ($K_{s\text{-total}}$) increases.

5.1. Prediction of penetration rate in the jointed rock mass

Since 1960, researchers had attempted to present models by investigating the effect of different parameters on the penetration rate. Some of the presented models included the geometric parameters of the Joint. These models are NTNU (Bruland, 1998)، QTBM (Barton, 2000)، Yagiz (2002،2008) ،Ramezanzadeh (2005،2008)، Gong and Zhao(2009) ،Khademi Hamidi et al (2010) ،Hassanpour et al(2010،2011) ،Farrokh et al(2012) ،Zare Naghadehi and Ramezanzadeh (2016) ،Alpine model (2016) Updated NTNU(Macias et al, 2017) ، and RJR model(2018) [11, 14,15, 16, 17, 18, 19, 20, 21, 22, 23, 24, 1, 12, 25]. NTNU model, which is obtained using empirical approaches, is generally used more than other ones, and its first presentation was in 1979 at the Norwegian University of Science and Technology. It has been reviewed and corrected according to the completion of the related information. The number of joints, spacing, and joint plane angle has been included in this model. The presented models are based on the rock classification systems where some geometrical characteristics and conditions of joints have entered these models indirectly [11]. One or both parameters of the joint plane angle and spacing have been included in other models. The number of joint sets and joint fractures as well as the two abovementioned parameters have been included in the RJR model [26].

5.2. Presentation of the model for predicting the penetration rate in the jointed rock mass

The investigations and analyses of the last section depict that both parameters of the joint persistence and volumetric joint count play a very important role in the penetration rate. In this research, having combined the joint geometric parameters and their relationship with the penetration rate, the Rock Joint Index (RJI) is defined as follows:

$$RJI = \left| \; 7.33(\alpha) - 8.17\ln\left(\frac{30.93J_V + 43.75Per}{14.7sp}\right) \right| \quad (3)$$

Where:

α is the angle between the tunnel axis and the planes of joint, J_v is the volumetric joint count, Per is joint persistence (meters), and Sp is joint spacing (meters). The convergence coefficient of this relationship is 0.83. Figure 10 shows the relationship between RJI and actual penetration rates.

The results of this relationship are compared to the actual penetration rate at 10 strokes, and at different lengths of the tunnel to investigate the accuracy of the RJI relationship. The geomechanical and operational parameters of the excavation in these tunnel sections have been given in Table 9.

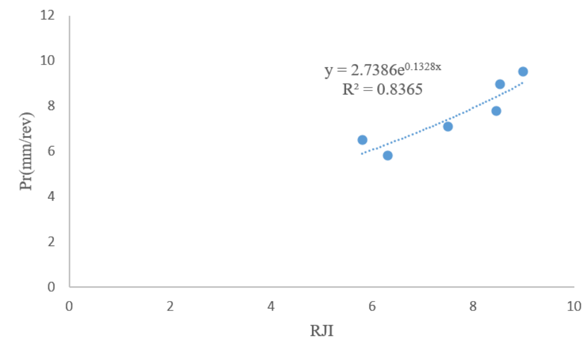

Fig. 10. Relationships between RJI with actual penetration rates

Table 9. Geomechanical Parameters of the sections of the tunnel

Rock group	Lithology	Number of boring strokes	Average Thrust (KN)	Average Torque	Penetration (mm/rev)	UCS(MPA)	Dip	Direction	Spacing (m)	Persistence (m)
RT3	Andesit-Basalt	566	3500	850	12	105	63	351	1.5	4
		874	4200	650	8.84	80	61	214	1.5	3
		1295	4400	650	7.87	160	48	218	1	4
		1712	4300	750	11	185	82	312	0.3	4
		3122	4850	860	9.5	180	81	308	0.8	4
RT1	Andesite	1496	5800	800	9.43	165	48	218	0.7	3
		2033	4250	800	9.31	170	73	359	0.3	1.5
		2303	4500	750	8.08	200	73	359	0.8	4
		2479	3900	859	10	175	8	375	0.9	3
		2980	4450	875	8.5	180	8	357	1.1	4

The difference between the actual penetration rate and RJI at each stroke has been shown in Figure 11.

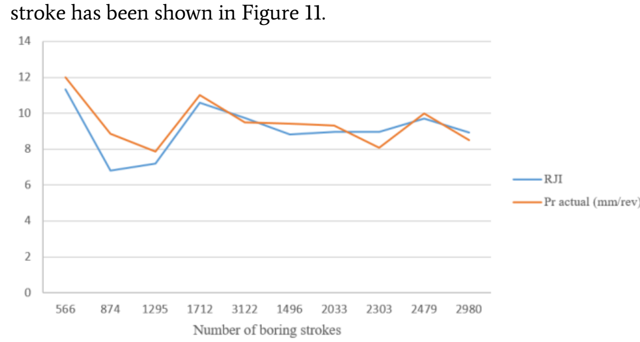

Fig. 11. RJI and actual penetration rate for each stroke

In continuation, the effect of uniaxial compressive strength (from the parameters of the intact rock) and two parameters of thrust and torque (from the machine operating parameters), as well as Pr, have been added to obtain a model to anticipate the penetration rate in the jointed rock mass.

$$\Pr_{RJI} = 1.49RJI + 7.34*10^{-5}\left(\frac{Thrust}{Torque}\right) - 0.024UCS \quad (4)$$

Where:

Thrust is in KN, torque is in KN-Meter, and uniaxial compressive strength (UCS) is in MPa. The convergence coefficient of this relationship is 0.88. In order to check the accuracy of the proposed model for predicting the penetration rate in the jointed rock mass, at 10 strokes and different lengths of the tunnel (Table 9), the results of this model have been compared with the actual penetration rate.

The relationship curves of the prediction model for the penetration rate of the jointed rock mass with the actual penetration rate have been shown in Fig. 12.

Fig. 12. PrRJI and Practual for strokes

6. Conclusion

Having studied the effect of each parameter on the penetration rate, it was concluded that only two parameters of the joint persistence and volumetric joint count have a direct relationship with the penetration rate. Generally, it can be stated that the two parameters of length and number of joints themselves play a very important role in the boreability of the jointed rock masses, and an increase in the amount of these two parameters will increase the boreability. Boreability of the rock mass depicts the interaction between the rock mass and cutting tool, and this is related to the effect of the joint parameters in the jointed rock masses. The fracturing factor which is a combination of two parameters (angle between the tunnel axis and the planes of joint and spacing joint) has an indirect relationship with the boreability. When the fracturing factor is classified based on the joint persistence, it is observed that the effect of the fracturing factor on the boreability increases as a result of the increase in the joint persistence. By investigating the effect of geometric parameters of the joint on the penetration rate, we have derived the rock joint index (RJI) model with a convergence coefficient of 0.83. After comparing the results of this model to the actual penetration rate, it was realized that this model has a good agreement with the actual penetration rates.

REFERENCES

[1] Wilfing, L. (2016). The Influence of Geotechnical Parameters on Penetration Prediction in TBM Tunnelling Hard Rock. Tehnische chnische university MÜNCHEN.

[2] Entacher, M. (2013). Measurement and interpretation of disc cutting forces in mechanized tunneling. Thesis, Technische Universität München.

[3] Gong, Q., Zhao, J. (2005). Numerical modeling of the effects of joint orientation on rock Fragmentation by TBM cutters. Tunnelling and underground space technology, Vol 20, PP I3-191.

[4] Paltrinieri, E. (2015). Analysis of TBM tunnelling performance in faulted and highly fractured rocks. Doctor of Philosophy thesis, EPFL.

[5] Sungong, C., Seungoong, L. (2015). Numerical Study to Estimate the Cutting Power on a Disc Cutter in Jointed Rock Mass. KSCE Journal of Civil Engineering.

[6] Gong, R., Jiao, Y. (2006). Numerical simulation of influence of joint spacing on rock Fragmentation by TBM cutters. Tunnelling and Underground Space Technology, 21 (1), 46–55.

[7] Sharifzadeh, M., Iranzadeh, A. (2009). Threedimensional numerical modelling of joint spacing and orientation effects on rock cutting process by a single TBM. Published in CIM Magazine, Vol 4, No 6.

[8] Bejari, H., Ataei, M., Khademi, J. (2011). Simultaneous effects of joint spacing and joint orientation on the penetration rate of a single disc cutter. Mining Science and Technology (China) 21(4):507-512.

[9] Bejari, H., Khademi, J. (2013). Simultaneous Effects of Joint Spacing and Orientation on TBM Cutting Efficiency in Jointed Rock Masses. Rock Mech Rock Eng, 46, 897–907.

[10] SOI Company. (2016). Engineering geological report of Kerman water conveyance tunnel. Unpublished report.

[11] Bruland, A. (1998). Hard Rock Tunnel Boring. Doctoral Thesis, Norwegian Institute of Technology, Trondheim

[12] Macias, F. (2016). Hard Rock Tunnel Boring Performance Predictions and Cutter Life Assessments. Thesis for the degree of Philosophiae Doctor, Norwegian University of Science and Technology.

[13] Bieniawski, Z.T. (1984). Rock mechanics design in mining and tunneling. A.A. Balkema, Rotterdam, 272 p.

[14] Barton, N. (2000). TBM Tunneling in Jointed and Fault Rock. Rotterdam: Balkema

[15] Yagiz, S. (2002). Development of rock fracture and brittleness indices to quantify the effects of rock mass features and toughness of the CMS model basic penetration for hard rock tunnel machines. Thesis Doctor of Philosophy, CSM.

[16] Yagiz, S. (2008). Utilizing rock mass properties for predicting TBM performance in hard rock conditions. Tunnel Underground Space Technology, 23(3):326–39.

[17] Ramezanzadeh, A., Rostami, J., Tadic, D. (2005). Influence of rock mass properties on Performance of hard rock TBMs. RETC PROCEEDINGS, Chapter 56.

[18] Ramezanzadeh, A., Rostami, J., Tadic, D. (2008). Effect of Rock Mass Characteristics on Hard Rock Tunnel Boring Machine Performance. 13th Australian Tunnelling Conference, Melbourne, VIC, 4 - 7 May.

[19] Gong, QM., Zhao, J. (2009). Development of a rock mass characteristics model for TBM penetration rate prediction. Int J Rock Mech Mining Sci 46(1):8–18.

[20] Khademi, J., Shahriar, K., Rezai, B., Rostami, J. (2010). Performance prediction of hard rock TBM using Rock Mass Rating (RMR) system. Tunnelling and Underground Space Technology, No. 25, pp. 333–345.

[21] Hassanpour, J. (2010). Analysis of actual TBM performance in Ghomrood project. Bulletin of Iranian Tunneling Association, No. 9, (article in Persian).

[22] Hassanpour, J., Rostami, J., Zhao, J. (2011). A new hard rock TBM performance prediction model for project planning. Tunnelling and Underground Space Technology, No. 26, pp. 595–603.

[23] Farrokh, E. (2012). Study of utilization factor and advance rate of hard rock TBMS. Doctor of Philosophy, Pennsylvania State University.

[24] Zare Naghadehi1, M., Ramezanzadeh, A. (2016). Models for estimation of TBM performance in granitic and mica gneiss hard rocks in a hydropower tunnel. Bull Eng Geol Environ.

[25] Rasouli, M. (2018). Rock Joint Rate (RJR); a new method for performance prediction of tunnel boring machines (TBMs) in hard rocks. Tunnelling and Underground Space Technology, 73 261–286.